Experimental Evidence for Dynamical Decay of Finite Nuclear Matter

R. Yanez, T. A. Bredeweg, E. Cornell,* B. Davin, K. Kwiatkowski,† V. E. Viola, and R. T. de Souza
Department of Chemistry and Indiana University Cyclotron Facility, Indiana University, Bloomington, Indiana 47405

R. Lemmon‡ and R. Popescu§
National Superconducting Cyclotron Laboratory and Department of Physics and Astronomy, Michigan State University, East Lansing, Michigan 48824
(Received 19 November 1998)

Ternary fission in the reaction $^{12}C + ^{232}Th$ at $E_{\mathrm{lab}} = 22A$ MeV reveals evidence for dynamical decay. The relative emission probability of intermediate-mass fragments (IMF: $3 \leq Z \leq 20$) as a function of the initial excitation of the composite system is examined. While IMFs emitted pre-scission exhibit behavior consistent with statistical emission, near-scission IMFs, characterized by unique angular and energy distributions, clearly exhibit a behavior consistent with dynamical decay. [S0031-9007(99)09056-0]

PACS numbers: 25.70.Jj, 25.70.Mn, 25.85.Ge

Nuclei are observed to decay via statistical emission of particles in a process analogous to evaporation in macroscopic liquids [1]. Nuclear collisions, used to prepare excited nuclear matter, may, however, lead to deformed nuclear shapes which are subject to dynamical instabilities [2]. Dynamical effects in nuclear reactions have been recognized in the preequilibrium emission of nucleons and fragments [3] and in the multifragmentation of the midrapidity zone in near-symmetric heavy-ion collisions [4]. All of these processes proceed on a rather fast time scale. The manifestation of dynamics on fragment emission on a longer time scale, e.g., the fission time scale, has not yet been reported. In this Letter we present the first clear experimental evidence of dynamical (nonstatistical) fragment decay on the fission time scale.

To study systems where the dynamical evolution of the shape of the nuclear system is important, yet keep the statistically thermalized energy modest, we have focused on ternary fission in the reaction $^{12}C + ^{232}Th$ at $E_{\mathrm{lab}} = 22A$ MeV. In this energy domain, incomplete fusion of the projectile and target nucleus occurs, followed by the fission of the heavy, excited composite system into two similar-sized fission fragments [5]. As the heavy composite nucleus undergoes the large scale deformation necessary for fission, it can decay via emission of neutrons, light charged particles ($1 \leq Z \leq 2$), and intermediate-mass fragments (IMF: $3 \leq Z \leq 20$). Such decay has been described with reasonable success within the framework of statistical emission theories [6,7]. Recently, it has also been found that IMFs are emitted from the region between the two fission fragments (neck) near the moment of scission, with characteristic energy and angular distributions [8,9]. The mechanism responsible for the production of these near-scission particles is presently unclear. Proposed mechanisms for similarly emitted alpha particles range from barrier modifications due to the proximity of the two fission fragments [10] to dynamical, double-neck rupture scenarios [11,12]. While the former scenario is still statistical—driven by phase space considerations—the latter scenario is largely, if not completely, dynamical.

The experiment was conducted at Michigan State University (MSU-NSCL). $A\,^{12}C$ beam accelerated by the K1200 cyclotron bombarded a self-supporting 700 $\mu g/cm^2$ ^{232}Th target. Fission fragments were detected in two hybrid large area multiwire proportional counters/parallel plate avalanche counters, spanning the laboratory polar angle range of $45° \leq \theta_A \leq 67°$ and $79° \leq \theta_B \leq 112°$ and centered at azimuthal angles of $\phi_A = 270° \pm 10°$ and $\phi_B = 90° \pm 10°$, respectively. These detectors were positioned ~30 cm from the target and provided an angular resolution of ~0.5°. The asymptotic velocity vectors of the fission fragments were deduced by using the measured position and the RF timing of the cyclotron. RF timing also aided in suppressing accidental coincidences in the analysis. IMFs were detected with five large area ionization chamber Si(IP)/CsI(Tl) telescopes. These telescopes, which provided identification of the Z, E, and θ of the IMFs with low detection thresholds ($E/A \geq 0.8$ MeV), were positioned in a group of four detectors centered at $\theta_{\mathrm{lab}} = 157°$, and a fifth detector positioned at $\theta_{\mathrm{lab}} = 100°$. The position of the group of the four detectors was roughly orthogonal to the line of separation of the fission fragments (scission axis). The 5 cm × 5 cm silicon detector in each telescope was segmented into four quadrants. Details regarding the performance of this type of detector have been previously published [13,14]. Both binary fission, corresponding to the detection of two fission fragments, and ternary fission, corresponding to the detection of two fission fragments and an accompanying IMF, were measured simultaneously. Geometrical efficiency corrections imposed by these coincidence requirements were performed.

The defining characteristics of IMF emission are summarized in Fig. 1. In Fig. 1a, the center-of-mass kinetic energy spectra of carbon fragments detected at $\theta_{\rm lab} = 157°$ (histogram) and $\theta_{\rm lab} = 100°$ (filled histogram) are shown. While the high-energy component is observed at both angles, the low energy component occurs only in the detectors positioned approximately orthogonal to the scission axis. Near-scission fragments are preferentially observed along this direction due to the focusing effect of the system's anisotropic Coulomb field. Their energies are significantly lower than those expected from the repulsion of a near-spherical source due to the near cancellation of the Coulomb field components parallel to the scission axis. Low energy fragments detected at backward angles are hence easily distinguished from any possible projectile remnants arising from a damped reaction on the basis of their kinetic energy and angular distributions. These features of near-scission emission have been well established in previous experiments [8,9]. The average value of the high-energy component peaks close to what would be expected in the statistical evaporation of a carbon fragment from a spherical Th-like nucleus (touching-spheres configuration). From here on, we distinguish between isotropic and near-scission emission based upon the center-of-mass kinetic energy of the IMF.

The dependence of the average kinetic energy on the Z of the emitted fragment is depicted in Fig. 1b. Both the isotropic and near-scission components exhibit a roughly linear dependence of the average energy on $Z_{\rm IMF}$. The solid line indicates the Coulomb barrier for a touching-spheres scenario given by

$$E_c = \frac{1.44 Z_{\rm IMF}(Z_{\rm source} - Z_{\rm IMF})}{1.4[A_{\rm IMF}^{1/3} + (A_{\rm source} - A_{\rm IMF})^{1/3}] + 2}\ {\rm MeV}, \tag{1}$$

where $Z_{\rm source}$ and $A_{\rm source}$ have been approximated by 90 and 232, respectively, to roughly account for incomplete fusion and pre-scission emission of nucleons. The kinetic energies for isotropically emitted fragments are roughly consistent with this simple formula, indicating that these fragments are emitted while the excited composite system is still relatively compact. Fragments emitted near scission have average kinetic energies significantly lower than those associated with statistical emission from a spherical source. This result is consistent with emission of the near-scission IMFs from a distended source as depicted in the cartoon of Fig. 1a.

The yield distributions of the isotropic and the near-scission components are shown in Fig. 1c. The isotropic component is well described by a power-law type behavior $Z^{-\tau}$ with $\tau = 3.1 \pm 0.2$. Near-scission emission has a much flatter Z distribution ($\tau = 1.3 \pm 0.1$), consistent with previous measurements [8,9], and for heavy IMFs ($Z \geq 8$) the yield distribution is essentially constant. A flatter yield distribution in a statistical emission framework is associated with higher excitation. Because of prior neutron emission and deformation, however, near-scission emission should be associated with lower excitation energy. Consequently, the flatter yield distribution for near-scission emission suggests a decay mode *not* solely dependent on excitation energy.

In order to understand the conditions under which fragments are emitted, we have examined the correlation between the fission-fragment folding angle and IMF emission yield. The folding angle technique has been well established as a means of deducing the linear momentum imparted to the fissile target nucleus [5], from which the resulting excitation of the composite system can be calculated. Binary fission following complete fusion would have an average folding angle of $\theta_{AB} = 152°$. In contrast, the most probable experimental folding angle in binary fission events associated with nonperipheral collisions is $\theta_{AB} = 157°$, consistent with the incomplete fusion of projectile and target nucleus in the formation of the composite system. In Fig. 2a the dependence of the folding angle on $Z_{\rm IMF}$ in ternary fission events is presented. For the isotropically emitted fragments (open symbols) the laboratory folding angle decreases monotonically with increasing $Z_{\rm IMF}$ due to the recoil imparted to the fissioning system by the backward emitted IMF. Since the angle, kinetic energy, and Z of the IMF are measured, the magnitude of this recoil can be calculated by assuming a Z/A ratio for the IMF, consistent with previous measurements [8,9]. The dashed line in Fig. 2a represents the folding angle associated with

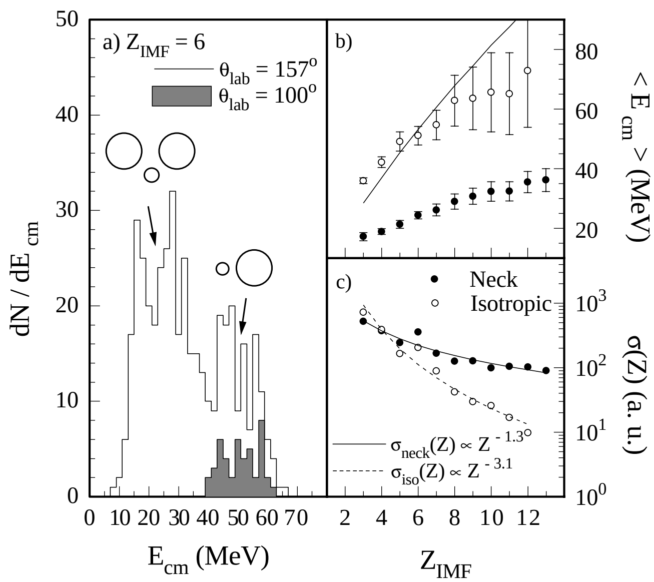

FIG. 1. (a) Kinetic energy distribution of carbon fragments in the center-of-mass of the fissioning composite system for detectors centered at $\theta_{\rm lab} = 157°$ (histogram) and at $\theta_{\rm lab} = 100°$ (filled histogram) in the reaction ^{12}C + ^{232}Th at $E_{\rm lab} = 22A$ MeV. (b) Average center-of-mass kinetic energy as a function of $Z_{\rm IMF}$ for neck (solid) and isotropic (open) emission. (c) Elemental yield distribution for neck (solid) and isotropic (open) emission.

87% linear momentum transfer of the projectile to the composite system, recoil of the fissioning system due to the IMF emission, and subsequent fission. The folding angle associated with isotropically emitted fragments can thus be understood within this picture. In contrast, neck IMFs exhibit a more complex behavior. While the folding angle for neck IMFs with $Z \leq 7$ also decreases monotonically, the folding angle for $Z \geq 8$ increases with increasing Z, indicating that the latter fragments are formed in events in which less linear momentum was initially transferred to the composite system.

We have determined the average fraction of the linear momentum transferred (FLMT) by the projectile to the composite system by iteratively correcting on an event-by-event basis the recoil of the backward emitted IMF. Its dependence on Z_{IMF} is shown in Fig. 2b. The isotropic fragments are associated with a nearly constant FLMT of 90% within the measurement uncertainties. The FLMT associated with neck-emitted IMFs decreases monotonically from 83% to 25% with increasing Z_{IMF}. Decreasing linear momentum transfer is associated with decreasing energy deposition in the composite system. Hence, the observed decrease in FLMT with the Z of the neck IMFs qualitatively suggests that neck emission of heavy fragments is *not* driven solely by excitation energy considerations. Sequential decay of a fission fragment (two-step fission) as a source of near-scission IMFs can, on average, be ruled out since the experimental mass distribution of fission fragments associated with near-scission emission is symmetric and independent of Z_{IMF}.

To explore the role of excitation energy on fragment emission we have constructed the yield ratios between different IMFs as a function of excitation energy. For statistically emitted fragments these ratios should manifest sensitivity to the IMF emission barriers. The average initial excitation of the composite system, $\langle E^* \rangle$, is calculated in the framework of an incomplete fusion model using the deduced FLMT,

$$\langle E^* \rangle = E_p \rho \frac{A_t}{A_t + \rho A_p} \sqrt{1 - \left(\frac{v_p}{c}\right)^2} + \langle Q \rangle , \qquad (2)$$

where E_p is the projectile energy, ρ is the FLMT, A_t and A_p are the mass numbers of the target and projectile, respectively, v_p is the velocity of the projectile, and $\langle Q \rangle$ is the average Q value of reaction channels consistent with the given ρ.

The dependence of the isotropic IMF yield relative to lithium on excitation energy is shown in Fig. 3. The experimental data exhibit an exponential increase with increasing excitation energy. This behavior can be qualitatively understood in terms of the Z dependence of the IMF emission barriers. Since the emission barrier increases with increasing Z_{IMF}, for a given excitation energy one observes a reduced emission probability for IMFs with larger Z. With increasing excitation energy this suppression in emission probability decreases.

We also compared the experimental data with the predictions of the statistical model SIMON [15]. The solid lines in Fig. 3 depict the predicted yields of Be, B, and C relative to Li fragments as a function of E^*/A. These relative yields have been renormalized for comparison with the data. The model semiquantitatively reproduces the main trend observed in the experimental data, showing a 3–4-fold increase in the relative yield over the measured excitation energy window. Thus, the behavior of isotropically emitted IMFs is consistent with statistical emission from a compact source.

The dependence of the relative yields of neck emission on the initial excitation of the system is shown in Fig. 4.

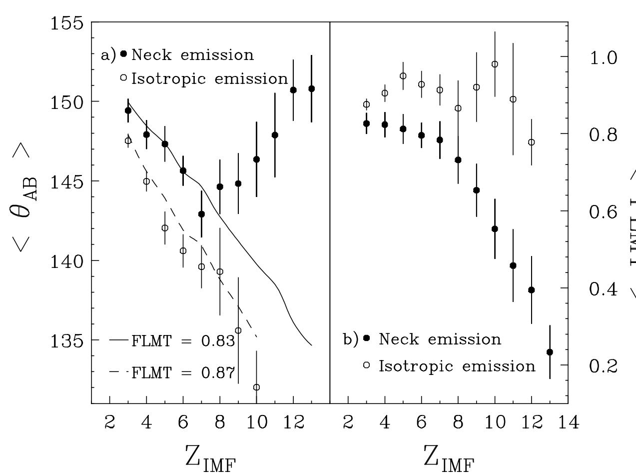

FIG. 2. (a) Z dependence of the average folding angle associated with neck and isotropic emission. (b) Z dependence of the average fractional linear momentum transfer for neck and isotropically emitted fragments.

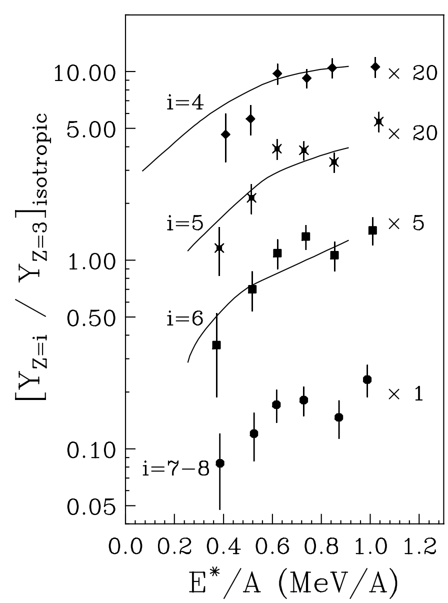

FIG. 3. Relative yield of various isotropically emitted IMFs as a function of excitation energy. Renormalized predictions of the statistical model SIMON are shown as solid lines.

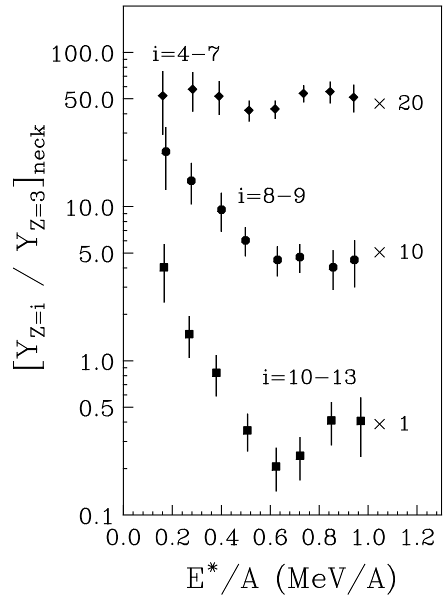

FIG. 4. Relative yield of various IMFs emitted from the neck region as a function of excitation energy.

The yields of neck-emitted fragments with $Z = 4-7$, $Z = 8-9$, and $Z = 10-13$ have been normalized by the yield of neck-emitted $Z = 3$ fragments. In marked contrast to the trends observed in Fig. 3, the relative yields in Fig. 4 do not show an exponentially increasing behavior with increasing excitation energy. For neck-emitted $Z = 4-7$ fragments the relative yield is approximately constant with increasing excitation energy. Such behavior could be understood if no emission barriers existed—consistent with emission of neck fragments from distended configurations. For $Z = 8-9$, however, the relative yield *decreases* with increasing excitation energy. A factor of 5 decrease is observed between the cases involving the lowest excitation (peripheral collisions) and cases involving the highest excitation (more central collisions). In the case of $Z = 10-13$, a suppression by a factor of approximately 20 is observed between $E^*/A = 0.2$ and $E^*/A = 0.6$. This behavior is inconsistent even with a zero emission barrier scenario and is a strong indication of a nonstatistical, dynamical origin of heavy fragment neck decay.

In understanding the association of significant heavy fragment neck yield with low linear momentum transfer, two points are noteworthy. First, for heavy fragments ($Z \geq 10$) the mass of the fragment approaches the mass of the neck. Thus, statistical emission from the neck would require evaporation of almost the entire "source" and is suppressed on the basis of source size effects. Suppression of statistical emission is important if one is to clearly isolate a coexisting/competing decay mechanism. Second, for collisions involving modest linear momentum transfer (25%), the deformation (stretching) introduced into the target nucleus may be significant. In contrast, central collisions should yield less deformation and greater heating of the system. Qualitative expectations dictate that survival of any initial stretching of the excited composite system into the fission channel results in a more elongated scission configuration and consequently a larger middle fragment. The survival of such an initial stretching should depend sensitively on the nature of nuclear dissipation. Preliminary calculations with a dynamical model of fission [16] bear out these qualitative expectations [17].

In conclusion, we have observed the existence of both statistical and nonstatistical (dynamical) emission of IMFs during fission. Dynamical emission of heavy fragments is enhanced for peripheral collisions for which initial deformation is expected to be large. General considerations dictate that the survival of dynamical stretching should depend sensitively on the magnitude and tensorial properties of nuclear dissipation. Dynamical production of fragments in ternary fission could thus serve as a sensitive probe of nuclear dissipation [16].

We acknowledge the assistance of the staff of the MSU-NSCL for providing the high quality beam for this experiment. We thank Dr. N. Cârjan and Dr. L. Phair for stimulating discussions on this topic. R. de Souza acknowledges the support of the Sloan Foundation. This work was supported by the U.S. Department of Energy under DE-FG02-92ER40714 (IU) and the National Science Foundation under Grant No. PHY-95-28844 (MSU).

*Present address: Lawrence Berkeley National Laboratory, Berkeley, CA 94720.
†Present address: Los Alamos National Laboratory, Los Alamos, NM 87545.
‡Present address: CCLRC Daresbury Laboratory, Warrington, WA4 4AD UK.
§Present address: Brookhaven National Laboratory, Upton, NY 11973.

[1] L. G. Sobotka *et al.*, Phys. Rev. Lett. **51**, 2187 (1983).
[2] D. L. Hill and J. A. Wheeler, Phys. Rev. **89**, 1102 (1953).
[3] J. Zhang *et al.*, Phys. Rev. C **56**, 1918 (1997).
[4] J. Tõke *et al.*, Phys. Rev. Lett. **77**, 3514 (1996).
[5] V. E. Viola, Nucl. Phys. **A471**, 53c (1987).
[6] M. Thoennessen, Nucl. Phys. **A599**, 1c (1996).
[7] D. Hilscher *et al.*, Phys. At. Nucl. **57**, 1187 (1994).
[8] D. E. Fields *et al.*, Phys. Rev. Lett. **69**, 3713 (1992).
[9] S. L. Chen *et al.*, Phys. Rev. C **54**, R2114 (1996).
[10] B. Lindl *et al.*, Z. Phys. A **328**, 85 (1987).
[11] U. Brosa *et al.*, Phys. Rep. **197**, 167 (1990).
[12] V. A. Rubchenya *et al.*, Z. Phys. A **329**, 217 (1988).
[13] K. Kwiatkowski *et al.*, Nucl. Instrum. Methods Phys. Res., Sect. A **299**, 166 (1990).
[14] D. Fox *et al.*, Nucl. Instrum. Methods Phys. Res., Sect. A **368**, 709 (1996).
[15] D. Durand (unpublished).
[16] N. Cârjan *et al.*, Nucl. Phys. **A452**, 381 (1986).
[17] N. Cârjan (private communication).